

**Titre:** Testing and modeling the compressibility of crushable rockfill based on particle scale descriptors

**Auteurs:** Chistian Maurer, Carlos Ovalle, & Esteban Saez

**Date:** 2025

**Type:** Communication de conférence / Conference or Workshop Item

**Référence:** Maurer, C., Ovalle, C., & Saez, E. (septembre 2025). Testing and modeling the compressibility of crushable rockfill based on particle scale descriptors [Communication écrite]. 78th annual CGS Conférence & 9th Canadian Permafrost Conference (Geo Manitoba 2025), Winnipeg, Manitoba, Canada (7 pages).  
Citation: <https://publications.polymtl.ca/70079/>

## Document en libre accès dans PolyPublie

**URL de PolyPublie:** <https://publications.polymtl.ca/70079/>  
PolyPublie URL:

**Version:** Version soumise à l'éditeur / Submitted version  
Révisé par les pairs / Refereed

**Conditions d'utilisation:** Tous droits réservés / All rights reserved  
Terms of Use:

## Document publié chez l'éditeur officiel

**Nom de la conférence:** 78th annual CGS Conférence & 9th Canadian Permafrost Conference  
Conference Name: (Geo Manitoba 2025)

**Date et lieu:** 2025-09-21 - 2025-09-25, Winnipeg, Manitoba, Canada  
Date and Location:

**Maison d'édition:**  
Publisher:

**URL officiel:**  
Official URL:

**Mention légale:**  
Legal notice:

# Testing and modeling the compressibility of crushable rockfill based on particle scale descriptors



Cristian Maurer<sup>1-2-3</sup>, Carlos Ovalle<sup>1-2</sup> & Esteban Saez<sup>3</sup>

<sup>1</sup> *Dép. des génies civil, géologique et des mines, Polytechnique Montréal*

<sup>2</sup> *Institut de recherche en mines et environnement (IRME) UQAT-Polytechnique, Québec, Canada*

<sup>3</sup> *Dep. of Structural and Geotechnical Engineering, Pontificia Universidad Católica de Chile, Santiago, Chile*

## ABSTRACT

Granular soils are susceptible to mechanical degradation due to particle crushing. This phenomenon can cause significant settlements in rockfill dams, mine waste rock piles or railway ballast. The effects of particle crushing can be captured by phenomenological constitutive models assuming a continuous media, even if breakage mechanisms occur at the grain scale. Therefore, to enhance those models, a better understanding of the links between micro- to macro-mechanical behavior is required. The main objective of this study is to develop a virtual test that can replicate the macro behavior of crushable rockfill by calibrating exclusively grain scale mechanical and geometrical properties. This will allow a deeper understanding of the multi-scale mechanisms governing the response of crushable coarse soils. Large oedometer tests on coarse crushed rock were conducted, as well as crushing tests on individual rock grains. In parallel, micro-mechanical simulations were performed in a virtual version of the laboratory specimen using the discrete element method (DEM). Digital realistic particle shapes were obtained from micro-CT scans, and particle breakage was simulated with the bonded cell method after calibration using crushing tests on individual grains. The results show that, as particle crushing increases during oedometric loading, the material becomes more compressible. The DEM numerical simulations can accurately replicate the experimental behavior and the evolution of grading upon crushing, by numerically reproducing the initial conditions of grading, characteristic grain shape, rock crushing strength and interparticle friction coefficient.

## RESUMÉ

Les sols granulaires sont sensibles à la dégradation mécanique due à la rupture des particules. Ces effets peuvent provoquer des tassements importants des barrages en enrochements, des haldes à stériles miniers ou des ballast ferroviaire. Les effets de la rupture des grains peuvent être capturés par des modèles constitutifs phénoménologiques supposant un milieu continu, même si les mécanismes de rupture se produisent à l'échelle des grains. Par conséquent, pour améliorer ces modèles, une meilleure compréhension des liens entre les comportements micro- et macro-mécaniques est nécessaire. L'objectif de cette étude est de développer un essai numérique capable de reproduire le comportement d'un enrochement en calibrant exclusivement les propriétés mécaniques et géométriques à l'échelle des grains. Ceci permettra d'obtenir une compréhension approfondie des mécanismes multi-échelle qui dominent le comportement. Des essais œdométriques de grande taille sur de la roche concassée grossière ont été réalisés, ainsi que des essais d'écrasement sur des grains de roche. En parallèle, des simulations micro-mécaniques ont été réalisées sur une version virtuelle de l'éprouvette de laboratoire par la méthode des éléments discrets (DEM). Des formes numériques réalistes de particules ont été obtenues à partir de scans micro-CT, et la rupture des particules a été simulée par la méthode des cellules cohésives, calibrée avec des essais d'écrasement sur des grains individuels. Les résultats montrent que, lorsque la rupture des grains augmente sous l'effet de la charge œdométrique, le matériau devient plus compressible. Les simulations numériques DEM permettent de reproduire avec précision le comportement expérimental et l'évolution de la granulométrie, en reproduisant numériquement la granulométrie initiale, la forme caractéristique des grains, la résistance à l'écrasement de la roche et le coefficient de frottement entre les grains.

## 1 INTRODUCTION

Empirical evidence has shown that the yielding of rockfills is strongly associated with the onset of particle crushing (Marsal, 1967; Alonso et al., 2016; Osses et al., 2024). Numerous constitutive models have incorporated breakage dependent hardening to capture the mechanical behavior of crushable materials (Daouadji & Hicher, 2010; Kikumoto et al., 2010; Ovalle & Hicher, 2020). However, deeper knowledge on the occurrence and evolution of grain crushing events at the particle scale could support the enhancement of continuous models, particularly on compressibility and yielding triggered by particle crushing.

This paper presents a multi-scale numerical test on crushable rockfill under compression. The aim is to capture the mechanical behavior of rockfill specimens by calibrating only particle scale properties, to get a deeper understanding of the multi-scale mechanisms governing the response.

Several studies have demonstrated that the statistics of individual rock particle crushing strength follow a Weibull distribution (Weibull, 1939; Lim et al., 2004), which captures scattering on particle strength. Moreover, scattering also strongly depends on particle size and particle shape (Ovalle & Dano, 2020). Based on this evidence, we hypothesize that a model with representative geometrical (i.e., size and shape) and mechanical (i.e.,

strength) descriptors at the grain scale, should be able to capture the macro-mechanical compressibility of a crushable rockfill.

We performed 300 mm diameter oedometric compression tests on dry rockfill. Grain characterization includes grading, particle shapes and crushing strength on a large number of particles. Particles were scanned and numerically reproduced in a discrete element method (DEM) simulation of crushable grains. The results of the DEM virtual oedometric specimen (i.e., a numerical version of the physical specimen) are compared against the large oedometric laboratory test.

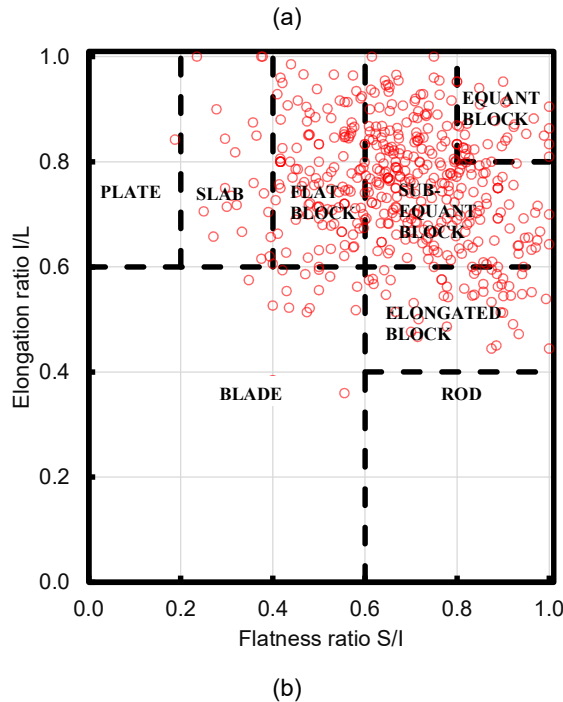
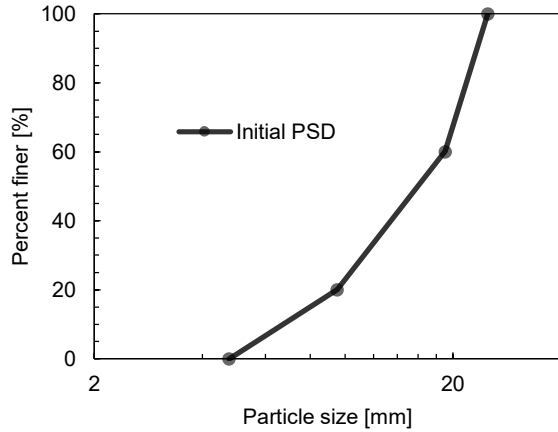


Figure 1. Rockfill properties: (a) particle size distribution and (b) characteristic particle shapes of the rockfill material.

## 2 EXPERIMENTAL METHODS

### 2.1 Rockfill

Quarry rockfill with maximum particle size of 25 mm and the particle size distribution (PSD) shown in Figure 1a was used for the testing program. The material has a uniformity coefficient of  $C_u=2.7$  and classifies as GP in the U.S.C.S.. Figure 1b presents the characteristic grain shapes of the angular crushed rock particles, obtained using manual caliper measurements on 600 particles. Moreover, as shown in Figure 2 detailed shapes of selected 18 grains were analyzed using digital images obtained with micro computed tomography scans; 6 grains from each size fraction : 19-25 mm, 9.5-19 mm and 4.75-9.5 mm.



Figure 2. Scanning rock particles for shape assessment.

### 2.2 Particle crushing strength

100 dry grains from each of the 3 size fractions were compressed individually until breakage between rigid parallel platens at constant compression rate of 0.03 mm/s (see Figure 3), i.e., carrying out lump tests. A Weibull statistical analysis was performed on the crushing strength data. The number of fragments after breakage was quantified and grouped by size fraction.

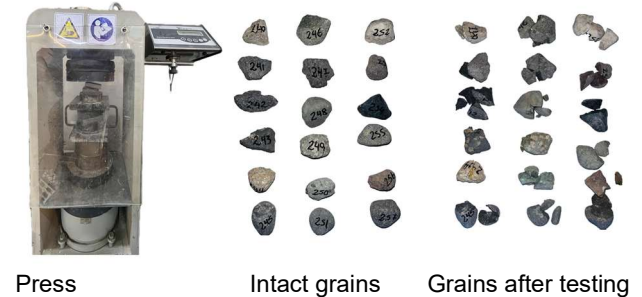


Figure 3. Individual particle crushing tests.

### 2.3 Large oedometric tests

A large oedometer device for specimens of 300 mm in diameter and 200 in height was used to compress dry specimens of the rockfill material. Figure 4 displays the oedometric cell installed under a frame with a hydraulic jack to apply vertical loads. The vertical displacement was monitored with an LVDT sensor. The maximum capacity of the device is 4,000 kPa of vertical stress, and the largest displacement is 50 mm.

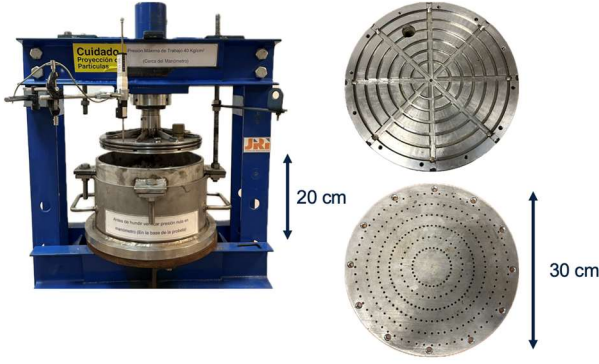


Figure 4. Large oedometric device.

Oedometric specimens were prepared by simply pouring the material (without compaction) to reach an initial void ratio  $e=0.6$ . Vertical stresses applied were of 10-25-50-100-200-400-800-1,600-3,200 kPa; each stress level was maintained for 24 hours. After the tests, the material was sieved to assess the amount of particle breakage.

### 3 NUMERICAL MODELING

The DEM numerical model is based on the Contact Dynamics method, implemented in the code LMGC90 (Dubois et al, 2018). The method considers perfectly rigid particles (i.e., there is no need to calibrate grain stiffness) and solves the equations of motion using an implicit time-stepping scheme that incorporates the kinematic constraints of frictional contact interactions.

Each scanned grain is first smoothed to avoid concavities. This simplifies the grain shape, while significantly reducing the computation time. The virtual particles are formed by potential fragments (or cells) using the bonded-cell method, where the scanned grain geometry is divided into a set of cells joined by an adhesive contact law (Cantor et al, 2022; Cardenas-Barrantes & Ovalle, 2025). Cells are generated using a centroidal tessellation using the software NEPER (Quey et al., 2011). To capture size effect on grain strength, the number of cells per unit of volume increases with the size of the grains: 5 cells were used for the particles in the size fraction 4.75-9.5 mm; 6 cells in fraction 9.5-19 mm; and 7 cells in the coarsest fraction 19-25 mm. The centroidal tessellation was used for the particle subdivision.

The cells within each particle were bonded by an adhesive strength  $\sigma_c$  (Huillca et al., 2021; Cantor et al., 2022). Bonds between cells crush when local stress exceeds  $\sigma_c$ . The contact law is based on pure cohesive Mohr-Coulomb failure criterion, which cohesion  $\sigma_c$  (i.e., adhesion) between cells.  $\sigma_c$  was varied to fit the experimental results of the single particle crushing tests.

#### 3.1 Single particle crushing virtual test

Numerical simulations of compression tests were performed on 100 virtual particles. The top platen applied vertical displacement at a constant rate of 0.03 mm/s until the grain breaks into two or more cells (see Figure 5).  $\sigma_c$  was calibrated to fit the Weibull distribution of the

experimental crushing strength statistics. A time step ( $\Delta t$ ) of  $5e-5$  s was used for the simulation, with the total number of steps varying between 400,000 and 1,000,000, depending on the particle size.

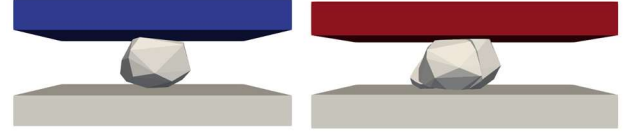


Figure 5. Individual particle crushing virtual test using DEM.

#### 3.2 Oedometric virtual test

The numerical oedometer test was conducted by replicating the laboratory initial grain size distribution using the scanned particles formed by bonded cells. The inter-particle friction coefficient used was 0.4. The procedure was divided into three phases, as shown in Figure 6. First, grains were enclosed within a spherical boundary and released from an initial height using an initial velocity of 0.01 m/s. In the second phase, a low constant stress of 1 kPa was applied to achieve an initial void ratio of  $e=0.6$ , consistent with the laboratory tests. By the end of this phase, the generated virtual granular specimen reached the minimum size criteria typically required for oedometer tests; namely, a base diameter at least ten times the diameter of the coarsest particle, and a height at least five times larger. Approximately 2,900 particles were required to meet these geometric conditions in the DEM virtual specimen. The third phase involved the application of the same loading sequence used in the laboratory tests. Compression was applied through the top platen under controlled loading conditions, with a total of 5,600 incremental time-steps per stress level and allowing the top platen to stabilize before advancing to the next stage. The time step used was the same as in the individual particle crushing simulations, i.e.  $5 \times 10^{-5}$  s. A total of 50,400 steps were executed to complete all loading stages.

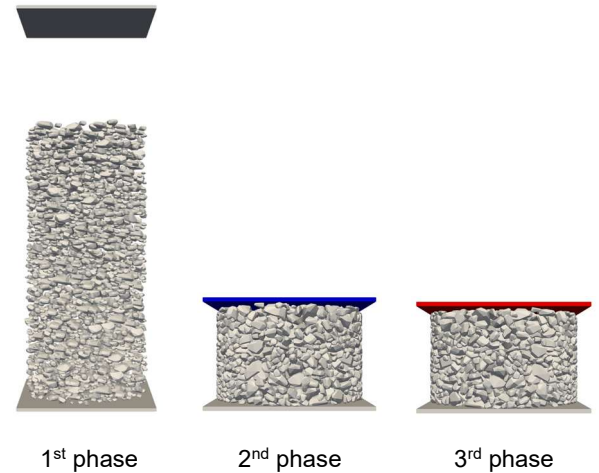


Figure 6. Numerical oedometric tests using DEM.

## 4 RESULTS

### 4.1 Statistical analysis of particles' crushing strength

The strength statistics of the individual grain crushing laboratory tests are presented in Figure 7a. Data is given as survival probability ( $P_s$ ) vs normalized stress, according to the Weibull distribution given by

$$P_s = \exp \left[ - \left( \frac{\sigma}{\sigma_o} \right)^m \right] \quad [1]$$

where  $\sigma$  is the induced tensile stress,  $\sigma_o$  is the characteristic grain strength at  $P_s = 0.37$ , and  $m$  captures particle strength variability; the higher the  $m$ , the lower the strength scattering. Figure 8 shows the Weibull parameters fitted to the experimental results (in black). Figure 7b displays the Weibull distribution after the DEM simulations of individual particle crushing tests. The best fit of the experimental results was found with  $\sigma_c = 55$  MPa. The calibrated Weibull parameters are similar to the ones from the experimental results, particularly  $\sigma_o$  depending on grain size (see red data in Figure 8). The  $m$  value from DEM is slightly lower than the value fitted to the laboratory tests, but still in the typical range of rock particles (Lim et al., 2004; Ovalle et al., 2014).

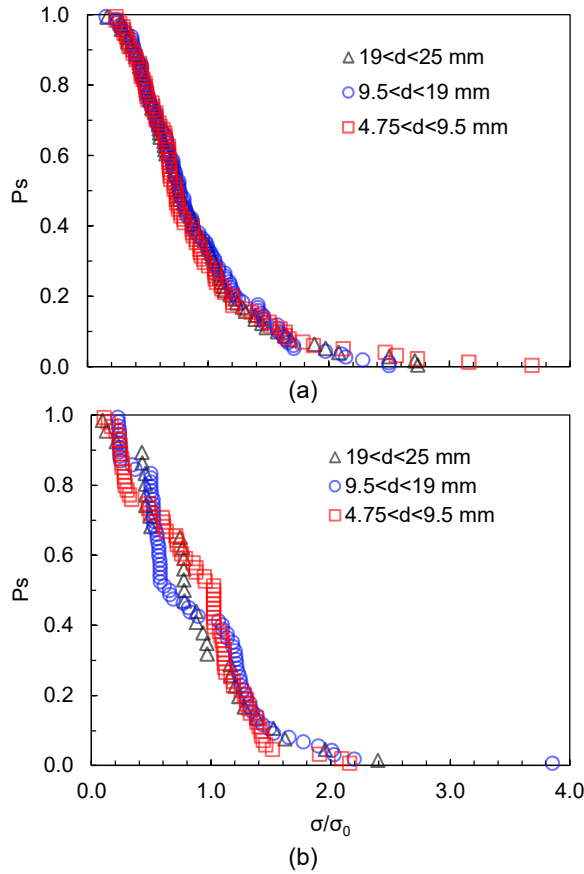


Figure 7. Particle crushing strength statistics: (a) experimental results and (b) DEM numerical simulations.

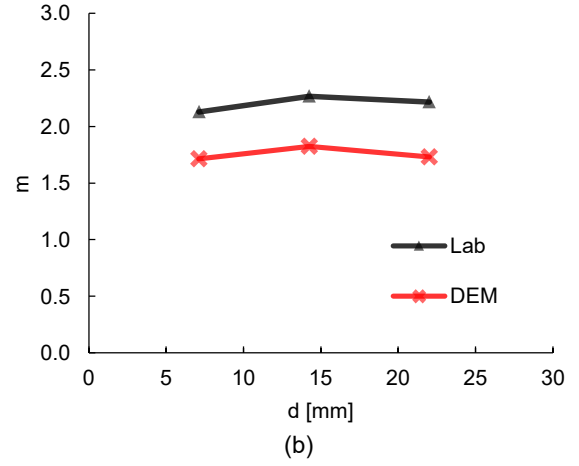
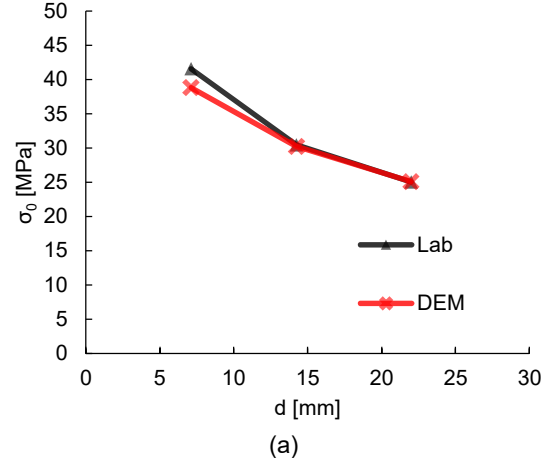
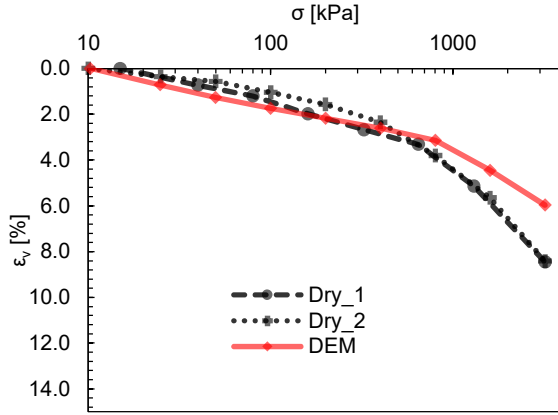


Figure 8. Weibull parameters (a)  $\sigma_o$  and (b)  $m$ , after the experimental tests and DEM numerical simulations.

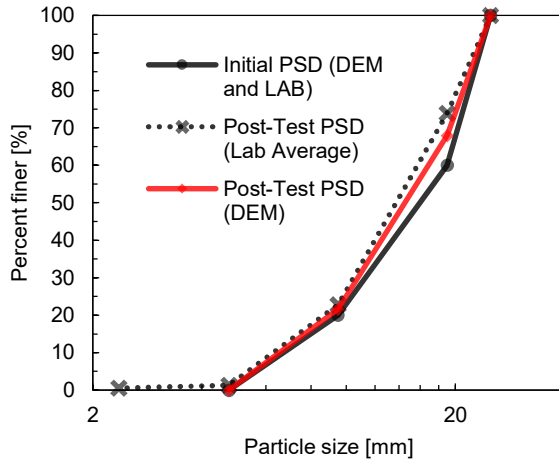
### 4.2 Oedometric tests

Figure 9 presents the results of two laboratory replicas (Dry\_1 and Dry\_2 in black) conducted under the same confining pressure, and a DEM numerical oedometer test (in red). Figure 9a shows the compressibility curves in terms of applied vertical stress ( $\sigma$ ) and volumetric strain ( $\epsilon_v$ ). The 2 laboratory tests exhibit similar behavior until the yielding point, at approximately  $\sigma=800$  kPa. Beyond yielding, compressibility increases significantly, presumably due to particle breakage. The virtual DEM test captures the general trend of the experimental data, including the yielding point. Thereafter, the virtual test follows a less compressible behavior. This mismatch might be explained by 2 main factors: (i) the numerical method does not consider grain elasticity and (ii) the damage of the loaded interparticle contacts is not simulated, which generates plastic deformation at the contact points. These issues could be addressed by a second order tessellation in smaller cells with higher  $\sigma_c$ , and are part of the perspectives of this work.

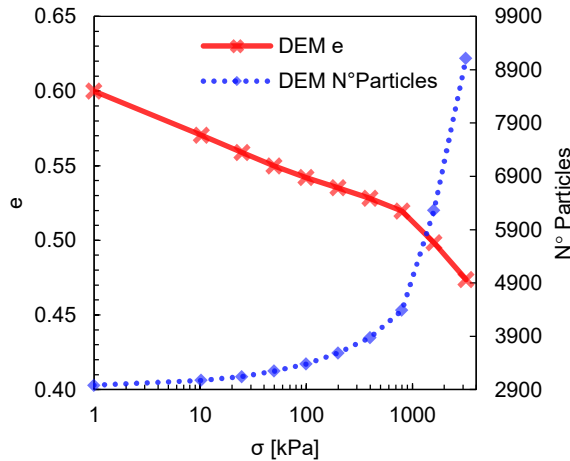




(a)



(b)



(c)

Figure 9. Experimental and numerical results for the (a) compressibility curves and (b) the PSDs before and after testing; (c) evolution of the number of particles with increasing stress in the DEM numerical test.

Figure 9b presents the evolution of the PSD before and after the tests. The DEM results closely match the average PSD measured after testing, indicating that the simulation captures particle breakage during loading. Figure 9c illustrates the variation of the void ratio and the number of particles in the DEM test as a function of the applied vertical stress. As the void ratio decreases progressively with loading, the number of particles increases in the numerical simulation, confirming that grain breakage contributes significantly to compression at high stresses. Moreover, yielding at 800 kPa coincides with a clear increasing rate of the number of particles. This observation confirms that yielding is triggered by higher rates of grain crushing events.

#### 4.3 Micro-mechanical description of the DEM test

To track contact evolution, the mechanical coordination number ( $Z_m$ ) is defined as the ratio between the number of active (i.e. transmitting force) contacts and the number of active particles; a particle is deemed active in force chains if it maintains three or more contacts. A pair of fragments is considered two separate particles once all cohesive contacts between them are broken.

Figure 10 presents the evolution of  $Z_m$  throughout the DEM loading path. After an initial rise due to initial grains rearrangement at low stress, the coordination remains nearly constant at  $Z_m=4.5$ , and then declines toward the end. The late stage decrease likely reflects increased particle breakage, which produces better graded material. It is assumed here that, after the first events of crushing, fine crushed fragments might rattle between coarse uncrushed particles. However, this is a transitional effect and further loading, crushing and rearrangement should increase  $Z_m$  at higher stresses.

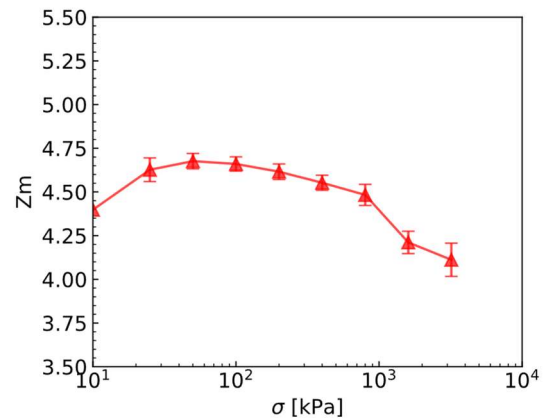


Figure 10. Evolution of the mechanical coordination ( $Z_m$ ) along the loading path (marks indicate mean values and bars are standard deviation during constant stress at each loading step).

Contact forces were examined through force-chain rendering to reveal the internal load-bearing network. Figure 11a couples these visualizations with probability-density functions (PDFs) for the contact forces at four key stress levels 400 kPa (pre-yield), 800 kPa (yield), and 1600

kPa and 3200 kPa (post-yield). The PDFs exhibit only minor changes, maintaining a similar slope and curvature across the loading stages, indicating that the overall force distribution remains stable even as stress increases. Figure 11b complements this analysis with a snapshot of the contact network inside the DEM specimen.

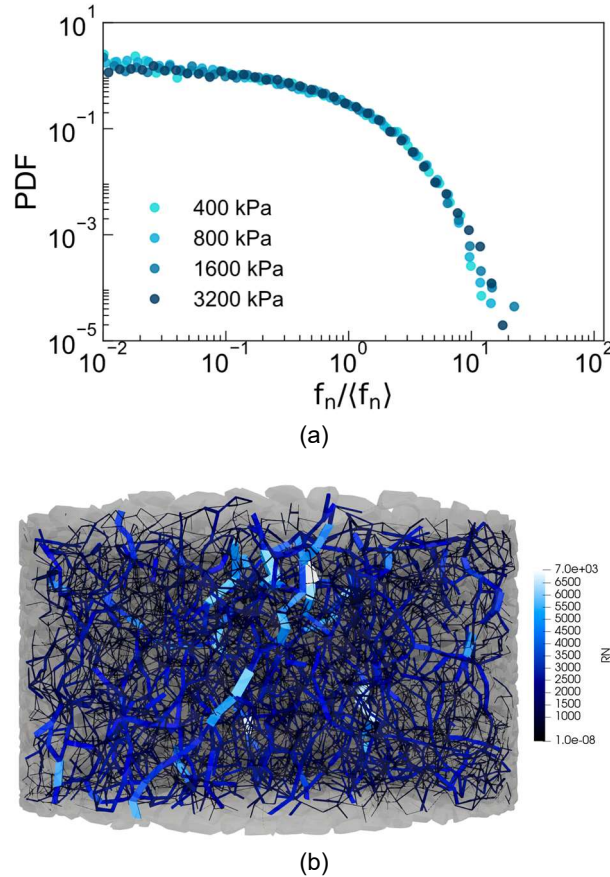


Figure 11. (a) probability-density function of the normal contact forces, normalized by the mean normal force in the DEM simulation; (b) contact-force network at the final loading stage, where line thickness is proportional to the magnitude of the normal force.

## 5 CONCLUSIONS

This study developed a multiscale numerical framework to investigate the compressibility of crushable granular materials, linking grain-scale descriptors with macroscopic behavior. By combining large-scale oedometric laboratory tests with discrete element method (DEM) simulations using realistic particle geometries and strengths, the proposed model demonstrates the feasibility of capturing complex mechanical responses through micro-mechanical calibration.

At the particle level, individual grain crushing tests were reproduced numerically using the bonded-cell method with centroidal tessellation. The numerical model closely

matched experimental observations of characteristic strength and variability across different particle sizes.

At the macro-scale, the virtual oedometric test successfully captured the stress-strain behavior of the material below the yielding stress. However, some differences appeared at higher stresses, where the DEM simulations underestimated compressibility compared to the laboratory results. These discrepancies are mainly attributed to limitations in the initial tessellation, which limits particle fragmentation and fines generation beyond the yielding threshold. However, the evolution of the particle size distribution in the simulations reasonably replicated the experimental trends. This supports the hypothesis that the formation of finer fragments due to intense particle breakage contributes to additional compressibility.

The micro-mechanical behavior shows no significant variation in the shape of the distribution of the normalized contact forces before and after yielding. This indicates that the force transmission within the granular assembly remains statistically similar across the yielding transition, suggesting that the force chains distribution and contact force heterogeneity are relatively unaffected by yielding. As particles break and their fragments are reclassified as individual particles, the number of contacts per particle decreases, resulting in a lower coordination number despite the increase in the total number of particles. This is likely due to small, crushed fragments rattling into large pores between coarser angular uncrushed grains. Certainly, at elevated stresses beyond the values used in this study, further particle crushing and rearrangement should promote a higher coordination number.

To enhance model fidelity at high stress levels, a perspective of this study is to implement a second-order tessellation beyond the yielding point. This refinement would allow for greater fragmentation potential and better alignment with experimental results, offering a promising pathway for future work in multiscale modeling of rockfill behavior. Also, the implementation of a time-dependent law for cell bonding cohesion could allow a multi-scale analysis of creep deformation due to delayed events of particle crushing, as reported in the literature (Oldecop and Alonso, 2007; Andò et al., 2019; Osses et al., 2021).

## 6 ACKNOWLEDGMENTS

This study benefited from financial support from the Natural Sciences and Engineering Research Council of Canada (NSERC) [project ALLRP 568607 – 21], the *Consortium de recherche et d'innovation en transformation métallique* (CRITM) [project 2021 – 068], *VRI Pontificia Universidad Católica de Chile* and the industrial partners of the *Institut de recherche en mines et environnement (IRME) UQAT-Polytechnique* (irme.ca/en).

## 7 REFERENCES

- Alonso, E., Romero, E., Ortega, E. 2016. Yielding of rockfill in relative humidity- controlled triaxial experiments. *Acta Geotechnica* 11(3), pp. 455–477.
- Andò, E., Dijkstra, J., Roubin, E., Dano, C., Boller, E. 2019. A peek into the origin of creep in sand. *Granular Matter* 21 (11), pp. 1–8.

- ASTM D2487-17, 2020. Standard Practice for Classification
- Cantor, D., Ovalle, C., Azéma, E. 2022. Microstructural origins of crushing strength for inherently anisotropic brittle materials. *International Journal of Solids and Structures* 238, 111399
- Cardenas-Barrantes, M., Ovalle, C. 2025. Multiscale Insights into Sliding Surface Liquefaction through DEM Simulations. *Computers and Geotechnics* 183, 107191
- Daouadji, A., Hicher, P.-Y. 2010. An enhanced constitutive model for crushable granular materials. *International Journal of Numerical and Analytical Methods in Geomechanics* 34 (6), 555–580.
- Dubois, F., Acary, V., Jean, M. 2018. The contact dynamics method: A non-smooth story. *Comptes Rendus Mécanique*, 346 (3), 247-262
- Huillca, Y., Silva, M., Ovalle, C., Carrasco, S., Quezada, J.C., Villavicencio, G. 2021. Modeling size effect on rock aggregates strength using a DEM bonded-cell model. *Acta Geotechnica* 16: 699–709
- Kikumoto, M., Wood, D.M., Russell, A. 2010. Particle crushing and deformation behaviour. *Soils and Foundations* 50 (4), 547–563.
- Lim, W.L., McDowell, G.R., Collop, A.C. 2004. The application of Weibull statistics to the strength of railway ballast. *Granular Matter* 6, 229–237.
- Marsal, R. 1967. Large-scale testing of rockfill materials. *Journal of the Soil Mechanics and Foundations Division ASCE* 93 (SM2), 27-44.
- Oldecop, L., Alonso, E., 2007. Theoretical investigation of the time dependent behavior of rockfill. *Géotechnique* 57 (3), pp. 289–301.
- Osses, R., Majdanishabestari, K., Ovalle, C., Pineda, J. 2021. Testing and modelling total suction effects on compressibility and creep of crushable granular material. *Soils and Foundations* 61, pp. 1581–1596.
- Osses, R., Pineda, J., Ovalle, C., Linero, S., Sáez, E. 2024. Scale and suction effects on compressibility and time-dependent deformation of mine waste rock material. *Engineering Geology* 340, 107668
- Ovalle, C., Frossard, E., Dano, C., Hu, W., Maiolino, S., Hicher, P.-Y. 2014. The effect of size on the strength of coarse rock aggregates and large rockfill samples through experimental data. *Acta Mechanica* 225(8), pp. 2199–2216
- Ovalle, C., Dano, C. 2020. Effects of particle size–strength and size–shape correlations on parallel grading scaling. *Géotechnique Letters* 10(2), pp. 191-197
- Ovalle, C., Hicher, P.-Y. 2020. Modeling the effect of wetting on the mechanical behavior of crushable granular materials. *Geosciences Frontiers* 11(2), pp. 487-494
- Quey, R., Dawson, P., Barbe, F. 2011. Large-scale 3D random polycrystals for the finite element method: Generation, meshing and remeshing. *Comput. Methods Appl. Mech. Eng.* 200 (17), 1729–1745
- Radjai, F. 2008. Contact dynamics method, *Eur. J. Environ. Civ. En.* 12, 871.
- Weibull, W. 1939. A statistical theory of the strength of materials. *Proceedings of Royal Swedish Institute of Engineering Research* 151.